Conducting properties of nanocomposite polymer electrolytes based on polyethylene glycol diacrylate and SiO$_2$ nanoparticles at the interface with a lithium electrode

G. R. Baymuratova, A. A. Slesarenko, A. V. Yudina, and O. V. Yarmolenko[★]
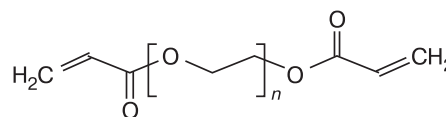
Institute of Problems of Chemical Physics, Russian Academy of Sciences,
1 prosp. Akad. Semenova, 142432 Chernogolovka, Moscow Region, Russian Federation.
E-mail: oyarm@icp.ac.ru

Nanocomposite polymer electrolytes based on polyethylene glycol diacrylate and 1 M LiBF$_4$ solution in γ-butyrolactone with addition of SiO$_2$ nanoparticles were synthesized and studied. Resistance measurement at the Li/electrolyte and Li/nanocomposite electrolyte interface by the time-resolved electrochemical impedance showed its significant decrease in the presence of SiO$_2$ nanoparticles. Charge-discharge cycling of prototypes of Li/LiFePO$_4$ batteries for 50 cycles also showed the advantage of using nanocomposite polymer electrolytes over electrolytes without SiO$_2$ additives.

Key words: nanocomposite electrolytes, polyethylene glycol diacrylate, LiBF$_4$, SiO$_2$ nanoparticles, ionic conductivity, lithium anode, impedance, Li/LiFePO$_4$ battery.

Nanocomposite polymer electrolytes (NPEs) comprise one of the promising classes of electrolytes for electrochemical devices, whose basic operating requirements are safety and flexibility.[1—3] The given class of polymer electrolytes was developed simultaneously with plasticized polymer electrolytes also referred to as gel electrolytes.[4,5] Further, these two classes of electrolytes converged as at the present time a polymer—salt composition is supplemented with an aprotic solvent to enhance the mobility of ions and nanoparticles (TiO$_2$, SiO$_2$, Al$_2$O$_3$, CeO$_2$, *etc.*) to increase the polymer matrix strength and absorptivity.[6—12] The given class of electrolytes is promising primarily for lithium and sodium electrochemical systems. Most NPEs are based on polymethyl methacrylate and polyvinylidene difluoride—hexafluoropropylene copolymer. The films of such electrolytes are prepared by means of solution casting technique. These NPEs principally differ from NPEs based on network polymers[13—19] synthesized from polyester diacrylates by a radical polymerization reaction. A 3D polymer network is cross-linked *via* a free-radical mechanism in (or without) a liquid organic electrolyte medium in the presence of inorganic nanoparticles. Benzoyl peroxide is used as a polymerization initiator. The synthesis features of a network NPE based on polyethylene glycol diacrylate (PEG-DA) and 1 M LiBF$_4$ solution in γ-butyrolactone (GBL) with SiO$_2$ nanoparticles (0—14 wt.%) were studied along with the physicochemical properties (conductivity and Young modulus) thereof as well as NPE film durability for 24 months.[20] High conductivity values (up to 4.5 mS cm^{-1}) at room temperature were recorded for

NPE with 6 wt.% SiO$_2$, and film durability was demonstrated for 2 years for a composition comprising 4 wt.% SiO$_2$ not losing the conducting properties. This result initiated an interest in the further studies to be carried out with the given NPE in electrochemical cells with lithium electrodes.

PEG-DA

Thus, the goal of this work is to study the compatibility of NPE based on PEG-DA, 1 M LiBF$_4$ solution in γ-butyrolactone, and SiO$_2$ nanoparticles with lithium electrodes and to carry out charge-discharge cycling with Li//LiFePO$_4$ battery prototypes comprising a nanocomposite electrolyte as compared to a polymer electrolyte free of added SiO$_2$ nanoparticles (hereinafter PE).

Experimental

Polyethylene glycol diacrylates, M$_n$ = 575 and 700 (Aldrich), were used.

Benzoyl peroxide (BP) (Aldrich) was purified by recrystallization from chloroform and further drying at room temperature first in air and then in vacuum. A 1 M LiBF$_4$ liquid electrolyte in γ-butyrolactone (Ecotech CJSC, Russia) with 0.008 wt.% water content was used. Aerosil SiO$_2$ nanoparticles (surface area 380 m^2 g^{-1}, average particle size 7 nm) had a hydrophilic porous surface, pH 3.6—4.3 (in 4% aqueous dispersion). Figure 1 rep-
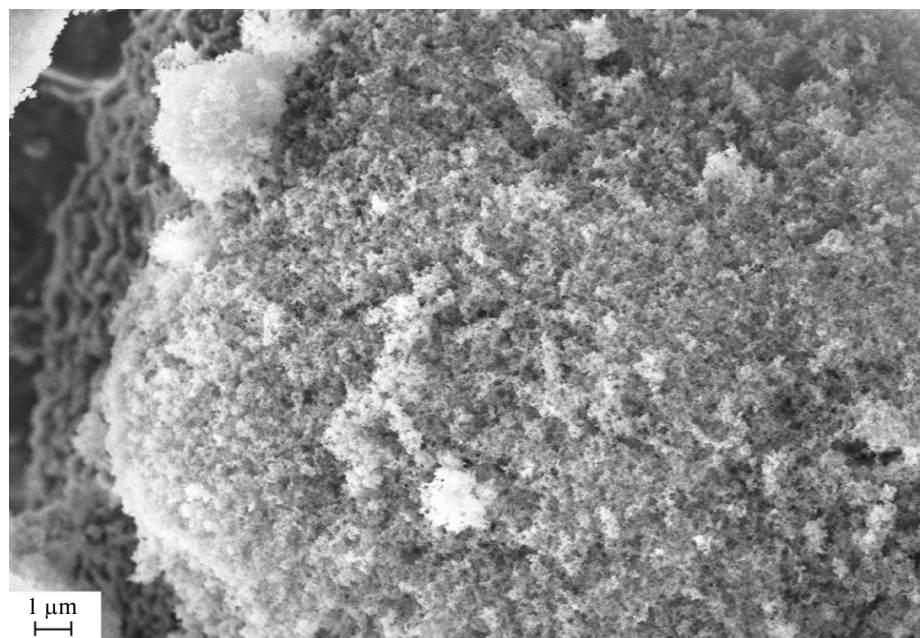
Fig. 1. Image of SiO$_2$ nanoparticle powder taken with a field emission scanning electron microscope.

resents a SiO$_2$ nanopowder image taken with a ZEISS LEO SUPRA 25 autoemission scanning electron microscope.

Synthesis of polymer electrolyte samples. The weighed sample of a PEG-DA oligomer (15 wt.%), a liquid electrolyte, and benzoyl peroxide (1 wt.%) were magnetically stirred for 30—60 min at 40°C until BP was completely dissolved, and a SiO$_2$ nanopowder was added. Then nanocomposite mixtures were treated by two following methods: (1) magnetic stirring at room temperature and (2) sonication for 20 s with a Bandelin Sonopul ultrasonic homogenizer (100 W) for a uniform distribution of SiO$_2$ nanoparticles in the system. Further sonication resulted in a partial polymerization of the mixture due to heating. Thus prepared nanocomposite mixtures were placed between two glasses (90×115 mm) treated with an antiadhesive solution. A technique of preparing a glass reactor for polymer electrolyte synthesis was already disclosed.[21] The mixture was cured according to the earlier used mode[20] as follows: 3 h at 60 °C, 1 h at 70 °C, 1 h at 80 °C, and 1 h at 120 °C. Thus prepared transparent films had a thickness of ~0.3 mm and maximum dimensions of 80×105 mm. The film dimensions and thickness are limited by the glass reactor dimensions and Teflon spacer thickness, respectively.

The NPE film conductivity measurements by means of electrochemical impedance used symmetric cells with stainless steel (SS) blocking electrodes having an area of 0.2 cm^2. The cell impedance was measured at 20 °C using an Electrochemical Instruments—Elinc Z-2000 impedance meter (Russia) at frequency range of $10-1 \cdot 10^5$ Hz at a signal amplitude of 10 mV.

The NPE//Li interface resistance *vs.* time was measured in sealed button cells with two lithium electrodes having an area of 2.27 cm^2.

The NPE film electrochemical stability window was voltammetrically recoded with an Elins P-8nano potentiostat in a Li/electrolyte/SS button cell, wherein a polymer electrolyte film without or with 6 wt.% SiO$_2$ added was placed between the lithium and SS electrodes.

Assembling and testing battery prototypes. A lithium foil (Lithium Element OJSC, Saratov) and LiFePO$_4$ (MTI Corp., USA) were used as electrode materials. Other cathode components were an HSV 900 polyvinylidene difluoride (PVDF) (Arkema, France) and a Timical Super C65 conducting carbon black (MTI corp., USA). The LiFePO$_4$ battery prototypes were assembled in laminated bags under argon in an MBraun (Germany) glove box using a Henkelman Minijambo (Netherlands) vacuum packer to seal the case; electrode dimensions were 1.5×1.5 cm. The cathode composition comprised 75 wt.% LiFePO$_4$, 20 wt.% carbon black, and 5 wt.% PVDF. All the components were dispersed in *N*-methylpyrrolidone to form a ~12% slurry, which was mechanically homogenized using an Isolab Light Duty (Germany) homogenizer for 10 min and further sonicated with a Sonopuls HD 3200 ultrasonic homogenizer (100 W) for 10 s. The cathode slurry was applied to an Al current collector (20 μm foil) and dried for 10 h at 120 °C. The amount of active substance on the electrode was 1.0—1.3 mg cm^{-2}.

The battery prototype charge-discharge cycling was carried out within the range of 2.6—3.8 V at a C/10 change current and a C/5 discharge current with a BTS-5V10mA 8-channel tester (Neware Technology Ltd., China).

Results and Discussion

To study a nanocomposite electrolyte compatibility with a lithium electrode, symmetric lithium cells with electrolyte compositions *1—3* (Table 1) were selected, and their impedances were measured during 1 year. Hereinafter, an additive-free polymer electrolyte was used as a reference sample.

Nanocomposite polymer electrolytes with minimum SiO$_2$ contents of 1 and 3 wt.% were selected to study the

Table 1. Components and conductivities of nanocomposite polymer electrolytes

Sample	Contents of electrolyte components (wt.%)				Electrolyte conductivity^a/S cm^{-1}
	PEG-DA	1 M LiBF$_4$ in GBL	SiO$_2$	BP	
1	15	84	0	1	$3.2 \cdot 10^{-3}$
2	15	83	1	1	$2.1 \cdot 10^{-3}$
3	15	81	3	1	$2.5 \cdot 10^{-3}$
4^b	15	78	6	1	$3.7 \cdot 10^{-3}$

^{a} At 20 °C.
^{b}Sample prepared after pre-sonication (see Experimental).

resistance of the solid electrolyte interphase (SEI) formed on the Li electrode surface. The conductivity of composites *2* and *3* (see Table 1) was near the first peak on the published conductivity curve *vs.* SiO$_2$ nanoparticle concentration (Fig. 2).[19] The methods of DSC and quantum-chemical modelling showed that 2 wt.% SiO$_2$ increases the number of charge carriers due to dissociation of the salt as a result of its interaction with the surface of SiO$_2$ nanoparticles.[19] The salt dissociation effect was further evidenced.[22] The second conductivity peak at 6 wt.% SiO$_2$ is due to the optimum ion transfer pathways created along the surface of SiO$_2$ nanoparticles.

Further studies[20] showed that if the mixture was stored or sonicated prior to film preparation, the first peak at 2 wt.% SiO$_2$ disappears (Fig. 3). The cause has not been completely studied. We can unambiguously note that the mechanism for the formation of the peak at 6 wt.% SiO$_2$ is quite stable and reproducible for all the nanocomposite electrolytes. In turn, the peak arising due to ionic dissociation is detected only in a few cases[23—27] characterizing primarily the systems with Aerosil 380 ultradispersed SiO$_2$ nanoparticles.

In view of the foregoing, PE and NPE with 1 and 3 wt.% SiO$_2$, which are most sensitive to SEI formation, were selected to study the NPE interaction with the lithium surface.
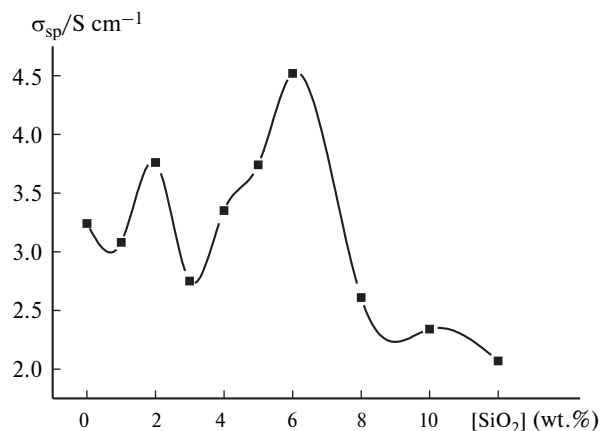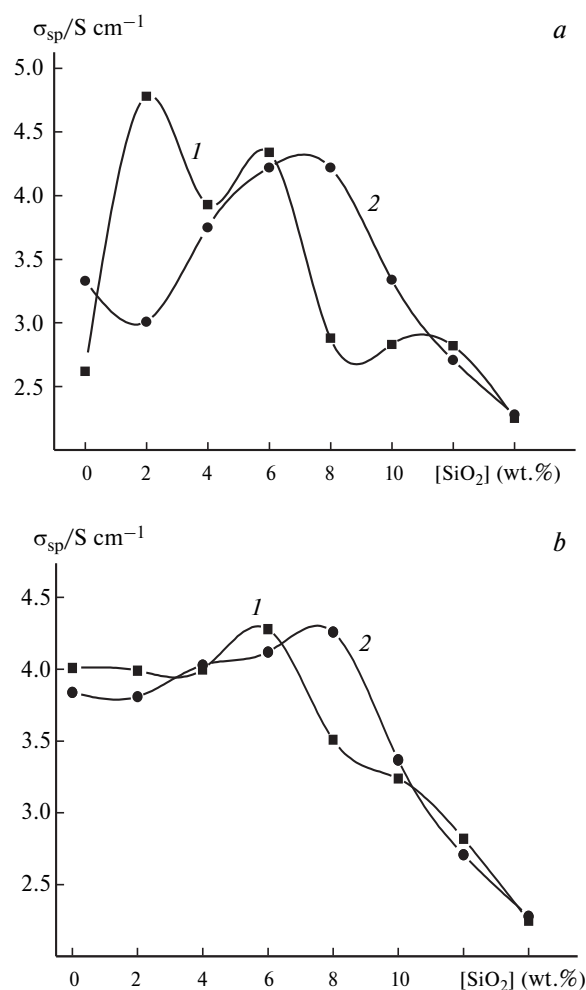
Figure 4 represents the impedance hodographs of the cells, wherein the electrolytes are PE and NPE with 1 and 3 wt.% SiO$_2$, recorded immediately upon assembling as well as on second, 9th, and 20th days, and after 1-year storage. Figure 4 shows that these hodographs are semi-

Fig. 3. NPE sample conductivity *vs.* SiO$_2$ nanoparticle content (PEG-DA 700). Cells were assembled immediately after synthesis (*a*) and after 1-week storage of films (*b*). *1*, Films synthesized without pre-sonication; *2*, films synthesized after pre-sonication of polymerization mixture.
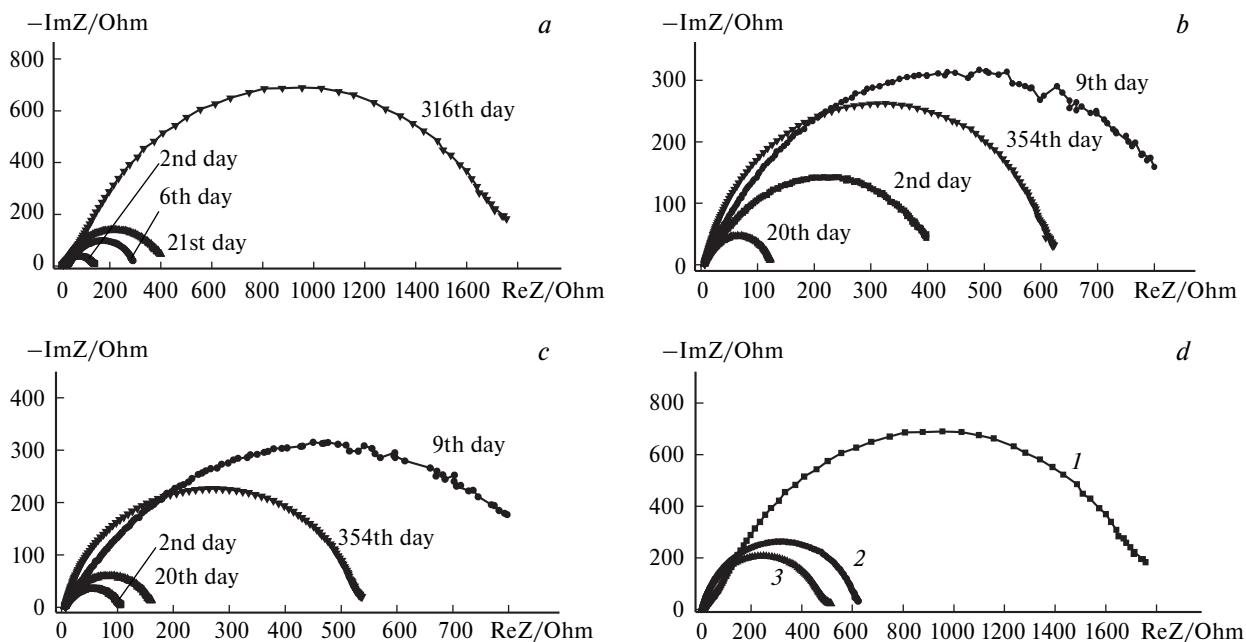

Fig. 2. Specific ionic conductivity ($\sigma_{sp.}$) *vs.* SiO$_2$ nanoparticle content (PEG-DA 575).[19]

Fig. 4. Impedance hodographs of Li//Li electrochemical cells, wherein electrolytes are PE (*a*) and NPE comprising 1 (*b*) and 3 wt.% SiO$_2$ (*c*) recorded on different days of storage, and hodographs of cells with PE (*1*) and NPE comprising 1 (*2*) and 3 wt.% SiO$_2$ (*3*) recorded upon 1-year storage (*d*).

circular that may correspond to the equivalent circuit represented in Fig. 5. Table 2 gives the equivalent circuit values calculated with ZView2 software for all the hodographs.

Table 2 shows that the electrolyte resistance (R_S) is virtually unchanged. An exception is the composite without SiO$_2$ additive on 316th day of storage, whose resistance increases by about four times, that is probably due to post-polymerization of the electrolyte. In the case of nanocomposite systems, no such increase in R_S occurs that evidences a positive influence of SiO$_2$ nanoparticles stabilizing the polymer matrix. The NPE films were also studied[20] after 2-year storage in a dessicator over P$_2$O$_5$. The PE films and NPE films with 2 wt.% SiO$_2$ "spread", and their conductivity could not be measured. Only a NPE sample with 4 wt.% SiO$_2$ retained all the mechanical and conducting properties.

In the present study, we assembled the sealed button cells, which can be stored for a long time.

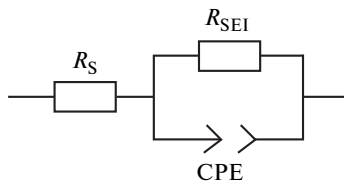Table 2 shows that the CPE-*P* values of the cells fall within the range of 0.70—0.89, while the CPE-*T* para-

meter, which may be attributed to the capacity of an electrical double layer, falls within the range of $(1.1—3.4) \cdot 10^{-5}$ F for all the systems. A special attention should be paid to the resistance (R_{SEI}) of the solid electrolyte layer on the Li electrode surface, which strongly depends on both the presence of SiO$_2$ and the storage time. Meanwhile, the composites with different SiO$_2$ contents exhibit different resistance *vs.* storage time curves that evidences the pro-

Table 2. Calculated equivalent circuit parameters (see Fig. 5) for Li/NPE/Li cells and composites with different SiO$_2$ contents on different days of storage

[SiO$_2$] (%)	Days	R_S /Ohm	CPE-$T \cdot 10^{-5}$ /F	CPE-P	R_{SEI} /Ohm
0	2	11	3.4	0.70	135
	6	8	1.8	0.70	840
	21	13	2.5	0.82	90
	316	55	1.2	0.82	1780
1	2	6	2.0	0.71	440
	9	5	1.1	0.74	930
	20	8	1.9	0.83	120
	354	7	1.7	0.87	630
3	2	5	2.8	0.76	105
	9	5	1.9	0.70	975
	20	6	1.7	0.81	160
	354	7	1.3	0.89	530

Fig. 5. Equivalent circuit of Li//Li cells, where R_S is electrolyte resistance, R_{SEI} is SEI layer resistance, CPE is a constant phase element.

Note. CPE-*P* is the phase shift constant, CPE-*T* is the electrical double layer capacitance.

cesses occurring at the interface. Thus, a PE cell (see Fig. 4, *a*) exhibits a direct relationship, *i.e.*, the resistance increases with the storage time and achieves the maximum value of 1780 Ohm on day 316. For a NPE, cell with 1 wt.% SiO_2 (see Fig. 4, *b*), SEI resistance on 9th day increased two-fold and amounted 930 Ohm, then it decreased to 120 Ohm on 20th day, and achieved the value of 630 Ohm after 1 year. An NPE cell with 3 wt.% SiO_2 shows a similar SEI forming process (see Fig. 4, *c*). For clarity, Fig. 4, *d* represents the hodographs of the PE and NPE cells comprising 1 and 3 wt.% SiO_2. Figure 4, *d* shows that a SiO_2 additive positively affects SEI formation, in particular, by structuring SiO_2 nanoparticles along the lithium surface. This effect was also observed by other researchers.[1,28]

The next stage involved the studies of lithium battery prototypes with the optimized composition of a nanocomposite electrolyte with 6 wt.% SiO_2, which is characterized by high conductivity and durability. First, we measured the upper limit of the electrochemical stability window of PE and NPE films with 6 wt.% SiO_2 in Li//SS cells. Then the voltammetric studies revealed the given value (against Li/Li^+) of 4.34 V for PE and 4.55 V for NPE with 6 wt.% SiO_2 (Fig. 6). Therefore, the added nanoparticles enhance the electrochemical stability of an electrolyte by 0.2 V.

We assembled the lithium battery prototypes with a $LiFePO_4$ cathode. The selected test NPE based on PEG-DA ($M_n = 575$) with 6 wt.% SiO_2 was prepared by sonicating the components of the mixture prior to the synthesis. Figures 7 and 8 represent the results, while Table 3 gives the electrochemical cell parameters and testing modes.

Figure 7 shows for the first charge-discharge cycle of PE and NPE, respectively, the charge plateau voltage of
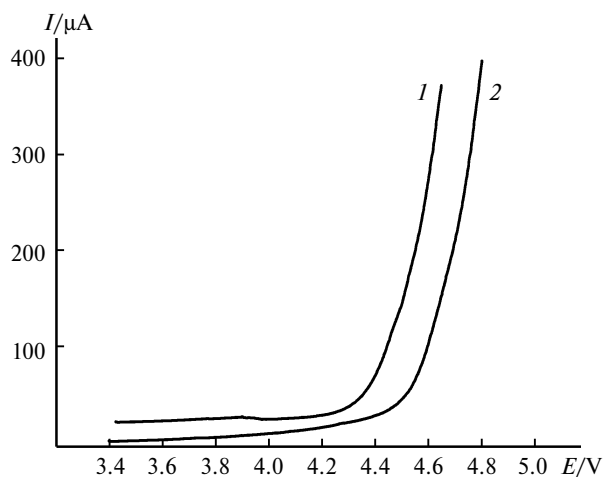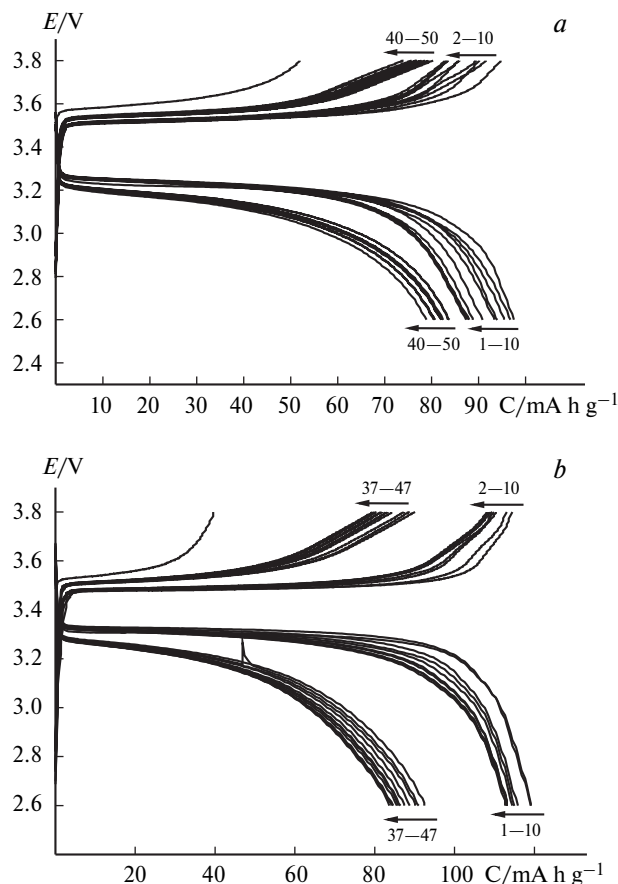
Fig. 7. Charge-discharge curves of $Li//LiFePO_4$ cells, wherein electrolytes are PE (*a*) and NPE with 6 wt.% SiO_2 (*b*). C/10 charge, C/5 discharge. Digits denote the numbers of charge and discharge curves, arrows indicate the order of numbering.

3.50 and 3.48 V and the discharge plateau voltage of 3.25 and 3.32 V. Thus, the difference between these plateaus is 0.24 V for PE and 0.16 V for NPE that is indicative of a positive effect of added SiO_2 nanoparticles on lithium dissolution from a lithium anode surface and intercalation thereof into $LiFePO_4$ olivine structure. The given tendency survives 50 charge-discharge cycles, and the difference between the plateau values amounts 0.34 and 0.23 V for PE and NPE cells, respectively.

Figure 8 shows that an NPE cell is characterized by a higher discharge capacity and Coulombic efficiency for 50 charge-discharge cycles. Meanwhile, PE exhibits the development effect for 10 cycles, whereas this process is not characteristic of NPE, which is indicative of good compatibility of the electrode/electrolyte interface. The general tendency of both cell types to degradation may be due to a relatively thick polymer electrolyte film (60—80 μm) as well as the presence of moisture in the radical polymerization step of electrolyte synthesis even if conducted in a sealed glass reactor. A higher capacity in the presence of nanoparticles was also observed in other studies using
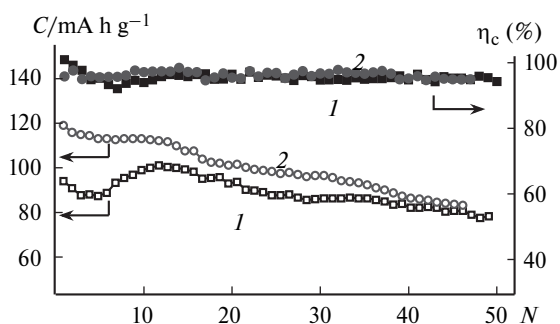
Fig. 6. Voltammograms of Li/electrolyte/SS cells, wherein electrolytes are PE (*1*) and NPE with 6 wt.% SiO_2 (*2*). Potential scan rate 2 mV s^{-1}; potential is given *vs.* Li//Li$^+$ pair.

Fig. 8. Discharge capacity (C) and Coulombic efficiency (η_c) of a Li//LiFePO$_4$ cell *vs.* charge-discharge cycle number (N) for Li//LiFePO$_4$ cells, wherein electrolytes are PE (*1*) and NPE with 6 wt.% SiO$_2$ (*2*).

the electrochemical Li//LiFePO$_4$,[29] C//LiFePO$_4$[11], and Li//LiCoO$_2$ systems.[30]

Therefore, for lithium electrochemical systems, we studied novel nanocomposite polymer electrolytes based on a 3D polymer network matrix of polyethylene glycol diacrylate formed by radical polymerization in a 1 M LiBF$_4$ electrolyte medium in γ-butyrolactone with added SiO$_2$ nanocomposite filler (Aerosil 380).

The SEI formation was studied on a lithium electrode surface in NPE cells with 1 and 3 wt.% SiO$_2$ added. The NPE film electrical resistance was shown stable for 1 year in sealed button cells, meanwhile the SiO$_2$-free polymer electrolyte resistance increases four-fold. Further, the electrochemical impedance method showed that the presence of SiO$_2$ nanoparticles in an electrolyte promotes a decrease in the electrical resistance at the electrolyte/Li interface that attests to the formation of conducting SEI. The comparative studies of Li//LiFePO$_4$ battery prototypes show of the advantages of using polymer electrolytes with nanoparticles.

Table 3. Electrochemical cell parameters and testing modes

Parameter	PE	NPE with 6 wt.% SiO$_2$*
Electrolyte film thickness/μm	79	60
Cathode thickness/μm	35	35
LiFePO$_4$ weight on electrode/mg cm^{-2}	1.3	1.0
Charging current density/μA cm^{-2}	21	16
Disharging current density/μA cm^{-2}	43	33
Charging time (C/10)/h	~5.0	~6.0
Discharging time (C/5)/h	~2.75	~3.3

* Composite was prepared after pre-sonication of the polymerization mixture (see Experimental).

References

1. O. V. Yarmolenko, A. V. Yudina, K. G. Khatmullina, *Russ. J. Electrochem.*, 2018, **54**, 325.
2. O. V. Yarmolenko, in *Nanostrurkurirovannye materialy dlya zapasaniya i preobrazovaniya energii* [*Nanostructured Materials for Energy Storage and Conversion*], Eds V. F. Razumov, M. V. Klyuev, Ivanovo State University, Ivanovo, 2009, 177 (in Russian).
3. O. V. Yarmolenko, A. V. Yudina, in *Organicheskie i gibridnye nanomaterialy: tendentsii i perspektivy* [*Organic and Hybrid Nanomaterials: Trends and Prospects*], Eds V. F. Razumov, M. V. Klyuev, Ivanovo State University, Ivanovo, 2013, 73 (in Russian).
4. L. Long, S. Wang, M. Xiao, Y. Meng, *J. Mater. Chem. A.*, 2016, **4**, 10038.
5. Yu. V. Baskakova, O. V. Yarmolenko, O. N. Efimov, *Russ. Chem. Rev.*, 2012, **81**, 367.
6. V. Aravindan, P. Vickraman, *Mater. Chem. Phys.*, 2009, **115**, 251.
7. V. Aravindan, P. Vickraman, T. P. Kumar, *J. Membr. Sci.*, 2007, **305**, 146.
8. D. Kumar, M. Suleman, S. A. Hashmi, *Solid State Ionics,* 2011, **202**, 45.
9. D. Kumar, S. A. Hashmi, *J. Power Sources*, 2010, **195**, 5101.
10. J. P. Sharma, S. S. Sekhon, *Solid State Ionics,* 2007, **178**, 439.
11. Y.-S. Lee, W.-K. Shin, J. Soo Kim, D.-W. Kim, *RSC Adv.*, 2015, **5**, 18359.
12. K. G. Khatmullina, G. R. Baimuratova, V. A. Lesnichaya, N. I. Shuvalova, O. V. Yarmolenko, *Polym. Sci., Ser. A*, 2018, **60**, 222.
13. C. Liao, X. G. Sun, S. Dai, *Electrochim. Acta*, 2013, **87**, 889.
14. N. Paranjape, P. C. Mandadapu, G. Wu, H. Q. Lin, *Polymer*, 2017, **111**, 1.
15. P. A. Golubev, G. Z. Tulibaeva, N. I. Shuvalova, O. V. Yarmolenko, *Moscow Univ. Chem. Bull.*, 2008, **49**, 324.
16. O. V. Yarmolenko, K. G. Khatmullina, L. M. Bogdanova, N. I. Shuvalova, E. A. Dzhavadyan, A. A. Marinin, V. I. Volkov, *Russ. J. Electrochem.*, 2014, **50**, 336.
17. O. V. Yarmolenko, A. V. Yudina, A. A. Marinin, A. V. Chernyak, V. I. Volkov, N. I. Shuvalova, A. F. Shestakov, *Russ. J. Electrochem.*, 2015, **51**, 412.
18. G. Z. Tulibaeva, A. F. Shestakov, A. V. Chernyak, V. I. Volkov, K. G. Khatmullina, A. V. Yudina, A. A. Ignatova, O. V. Yarmolenko, *Russ. Chem. Bull.*, 2016, **65**, 1951.
19. O. V. Yarmolenko, K. G. Khatmullina, G. R. Baimuratova, G. Z. Tulibaeva, L. M. Bogdanova, A. F. Shestakov, *Mendeleev Commun.*, 2018, **28**, 41.
20. A. V. Yudina, M. P. Berezin, G. R. Baymuratova, N. I. Shuvalova, O. V. Yarmolenko, *Russ. Chem. Bull.*, 2017, **66**, 1278.
21. A. V. Chernyak, M. P. Berezin, N. A. Slesarenko, V. A. Zabrodin, V. I. Volkov, A. V. Yudina, N. I. Shuvalova, O. V. Yarmolenko, *Russ. Chem. Bull.*, 2016, **65**, 2053.

22. N. Byrne, J. Efthimiadis, D. R. MacFarlane, M. Forsyth, *J. Mater. Chem.*, 2004, **14**, 127.
23. R. Kumar, S. S. Sekhon, *J. Appl. Electrochem.*, 2009, **39**, 439.
24. R. Kumar, *Indian J. Phys.*, 2015, **89**, 241.
25. J. P. Sharma, S. S. Sekhon, *Solid State Ionics*, 2007, **178**, 439.
26. D. Kumar, S. A. Hashmi, *J. Power Sources*, 2010, **195**, 5101.
27. G. P. Pandey, S. A. Hashmi, R. C. Agrawal, *Solid State Ionics*, 2008, **179**, 543.
28. B. Kumar, L.G. Scanlon, *J. Power Sources,* 1994, **52**, 261.
29. Y. Ma, L. B. Li, G. X. Gao, X. Y. Yang, Y. You, *Electrochim. Acta*, 2016, **187**, 535.
30. R. Zhou, W. Liu, X. Yao, Y. W. Leong, X. Lu, *J. Mater. Chem. A*, 2015, **3**, 16040.